PHYSICAL REVIEW D **95,** 115021 (2017)

Constraints of chromoelectric dipole moments to natural SUSY type sfermion spectrum

Nobuhiro Maekawa,[1,2,*] Yu Muramatsu,[3,†] and Yoshihiro Shigekami[1,‡]

[1]*Department of Physics, Nagoya University, Nagoya 464-8602, Japan*
[2]*Kobayashi Maskawa Institute, Nagoya University, Nagoya 464-8602, Japan*
[3]*Institute of Particle Physics and Key Laboratory of Quark and Lepton Physics (MOE), Central China Normal University, Wuhan, Hubei 430079, People's Republic of China*

(Received 24 February 2017; published 16 June 2017)

We investigate the lower bounds of sfermion masses from the constraints of chromoelectric dipole moments (CEDMs) in the natural SUSY-type sfermion mass spectrum, in which stop mass $m_{\tilde{t}}$ is much smaller than the other sfermion masses m_0. The natural SUSY-type sfermion mass spectrum has been studied since the supersymmetric (SUSY) flavor-changing neutral currents (FCNC) are suppressed because of large sfermion masses of the first two generations, and the weak scale is stabilized because of the light stop. However, this type of sfermion mass spectrum is severely constrained by CEDM, because the light stop contributions to the up quark CEDM are not decoupled in the limit $m_0 \to \infty$, while the down quark CEDM is decoupled in the limit. It is important that the constraints are severe even if SUSY-breaking parameters (and Higgsino mass) are taken to be real because complex diagonalizing matrices of Yukawa matrices, which are from complex Yukawa couplings, generate nonvanishing CP phases in off-diagonal elements of sfermion mass matrices. We calculate the CEDM of up and down quarks numerically in the minimal SUSY standard model, and give the lower bounds for stop mass and the other sfermion masses. We show that the lower bound of stop mass becomes 7 TeV to satisfy the CEDM constraints from Hg EDM. The result is not acceptable if the weak scale stability is considered seriously. We show that if the up-type Yukawa couplings are taken to be real at the grand unification scale, the CEDM constraints are satisfied even if $m_{\tilde{t}} \sim 1$ TeV.

DOI: 10.1103/PhysRevD.95.115021

I. INTRODUCTION

The supersymmetric (SUSY) extended standard model (SM) is one of the most promising candidates as the model beyond the SM. The minimal SUSY SM (MSSM) can realize the stability of the weak scale and provide a candidate of the dark matter. Moreover, it is consistent with the grand unified theory (GUT) [1] since the three gauge couplings meet at a scale which is called the GUT scale.

However, the supersymmetry must be broken because the supersymmetric partners of the quark and lepton, which are the squark and slepton, have not been found yet, and the scale is expected to be around the weak scale, not to destabilize the weak scale. Generically, the SUSY-breaking parameters which violate the flavor and CP symmetry induce too large flavor-changing neutral current (FCNC) processes (the SUSY flavor problem) and the CP-violating processes (SUSY CP problem). To avoid these problems, we usually assume the universal sfermion masses and/or real SUSY-breaking parameters at a scale. One more interesting possibility is the decoupling solution in which the SUSY-breaking scale is taken to be much higher than the weak scale. Then the SUSY contributions to the FCNC processes and CP-violating processes are suppressed by decoupling features. The sfermion masses are required to be $O(1000)$ TeV to sufficiently suppress the contribution to ϵ_K if off-diagonal elements of sfermion mass matrices are not suppressed [2]. This possibility has been examined more in detail since the observed Higgs mass 125 GeV [3] requires a higher SUSY-breaking scale [4]. Unfortunately, such higher SUSY-breaking parameters result in the destabilization of the weak scale; i.e., strong fine-tuning is needed to obtain the weak scale.

One possible way to improve the fine-tuning is to make the stop mass lower, around 1 TeV, while the other scalar fermions (sfermions) have much larger masses than 1 TeV to suppress the FCNC and CP-violating processes. Such sfermion mass spectrum is called effective SUSY-type sfermion masses or natural SUSY [5]. Unfortunately, it has been pointed out that the sufficiently large sfermion masses are difficult to be taken since large sfermion masses and small stop mass at the GUT scale tend to result in negative stop mass square at the weak scale via two loop renormalization group effects. Large gluino mass can improve the situation, because it contributes to the stop mass square positively. Roughly, squark masses except stop mass must be smaller than 5 times gluino mass. Therefore,

*maekawa@eken.phys.nagoya-u.ac.jp
†yumura@mail.ccnu.edu.cn
‡sigekami@eken.phys.nagoya-u.ac.jp

if the gluino mass is around 2–3 TeV, which is target of LHC experiment, $O(10)$ TeV is the upper limit. Then, the off-diagonal elements of sfermion mass matrices must be suppressed. One way to suppress the off-diagonal elements is to require the modified sfermion universality in which all sfermion masses except third generation 10 dimensional fields of $SU(5)$ are universal at the GUT scale [6,7] as

$$\tilde{m}^2_{\mathbf{10}} = \begin{pmatrix} m_0^2 & 0 & 0 \\ 0 & m_0^2 & 0 \\ 0 & 0 & m_3^2 \end{pmatrix}, \qquad \tilde{m}^2_{\bar{\mathbf{5}}} = \begin{pmatrix} m_0^2 & 0 & 0 \\ 0 & m_0^2 & 0 \\ 0 & 0 & m_0^2 \end{pmatrix}. \tag{1}$$

Such mass spectrum can be naturally obtained in E_6 GUT [8–10] with family

symmetry [6]. Here the universality for all $\bar{\mathbf{5}}$ fields of $SU(5)$ is important to obtain sufficiently small FCNC processes even if the diagonalizing matrices for $\bar{\mathbf{5}}$ fields have large mixings. Therefore, when the diagonalizing matrices of 10 fields and $\bar{\mathbf{5}}$ fields of $SU(5)$ are estimated by Cabibbo-Kobayashi-Maskawa (CKM) matrix $V_{\rm CKM}$ and Maki-Nakagawa-Sakata (MNS) matrix $V_{\rm MNS}$ as

$$V_{\mathbf{10}} \sim V_{\rm CKM} \sim \begin{pmatrix} 1 & \lambda & \lambda^3 \\ \lambda & 1 & \lambda^2 \\ \lambda^3 & \lambda^2 & 1 \end{pmatrix}, \qquad V_{\bar{\mathbf{5}}} \sim V_{\rm MNS} \sim \begin{pmatrix} 1 & \sqrt{\lambda} & \lambda \\ \sqrt{\lambda} & 1 & \sqrt{\lambda} \\ \lambda & \sqrt{\lambda} & 1 \end{pmatrix}, \tag{2}$$

which are expected in some GUT models [10,11], off-diagonal elements of sfermion mass matrices can be suppressed as

$$\tilde{m}^2_{\mathbf{10}} = V^\dagger_{\mathbf{10}} \begin{pmatrix} m_0^2 & 0 & 0 \\ 0 & m_0^2 & 0 \\ 0 & 0 & m_3^2 \end{pmatrix} V_{\mathbf{10}} = m_0^2 \mathbf{1} + (m_3^2 - m_0^2) \begin{pmatrix} \lambda^6 & \lambda^5 & \lambda^3 \\ \lambda^5 & \lambda^4 & \lambda^2 \\ \lambda^3 & \lambda^2 & 1 \end{pmatrix} \tag{3}$$

and most of flavor and CP constraints can be satisfied. Lepton flavor violation processes like $\mu \to e\gamma$ or $\tau \to \mu\gamma$ may be seen [12] if $m_3 \sim O(100)$ GeV, but unfortunately, we lost the strong reason to take $m_3 \sim O(100)$ GeV after discovery of Higgs particle because lower bound of stop masses becomes around 1 TeV in the MSSM in order to realize the Higgs mass ∼125 GeV. Here $\lambda \sim 0.22$ is the Cabibbo mixing angle.

However, even if this modified universal sfermion mass spectrum with real SUSY-breaking parameters are adopted, the EDM constraints from the experimental bound [13] as

$$d_N < 3.0 \times 10^{-26}\ e\,\text{cm} \tag{4}$$

$$d_{Hg} < 7.4 \times 10^{-30}\ e\,\text{cm} \tag{5}$$

become severe. The essential point is that the sfermion mass matrices of **10** fields of $SU(5)$ in super-CKM basis where quark and lepton mass matrices are diagonal have complex off-diagonal elements generically unless sfermion masses are universal because Yukawa couplings are complex, and therefore, diagonalizing matrices are complex to obtain the Kobayashi-Maskawa (KM) phase. Therefore, the diagram with the complex off-diagonal elements can contribute to the (chromo) EDM, and give severe constraints to the off-diagonal elements [14]. Most of contributions to (chromo) EDM are decoupled in the limit $m_0 \to \infty$ with finite m_3, but some contributions to up quark (chromo) EDM are not decoupled in the limit [15]. The constraint becomes

$$\mathrm{Im}\left[\frac{(\tilde{m}^2_{\mathbf{10}})_{31}}{m_0^2}\frac{(\tilde{m}^2_{\mathbf{10}})_{13}}{m_0^2}\right] < \left\{\begin{matrix} 5.3\times10^{-6}(\mathrm{Hg}) \\ 1.6\times10^{-4}(\mathrm{neutron}) \end{matrix}\right\} \left(\frac{m_3}{2\,\mathrm{TeV}}\right)^2, \tag{6}$$

which are obtained by the mass insertion approximation (MIA)[16] with certain mass spectrum of SUSY particles. Here we have used the relations between neutron (Hg) EDMs and CEDM of quarks in Ref. [17]([18]) for neutron (Hg) EDM. Although the ambiguity in theoretical calculation of EDMs is large especially for Hg [18,19], we give the constraints to the model by neglecting the uncertainty in this paper. Since $(\tilde{m}^2_{\mathbf{10}})_{31}/m_0^2 \sim (\tilde{m}^2_{\mathbf{10}})_{13}/m_0^2 \sim \lambda^3$, the predicted EDM of Hg becomes about 20 times larger than the experimental bound even if we take stop mass $m_{\tilde{t}} \sim 2$ TeV and the diagonalizing matrices of $V_{\mathbf{10}}$ have small mixings like CKM matrix. This severe constraint looks to be general for almost all models with natural SUSY spectrum, and it is important to study the solution to this problem if natural SUSY spectrum is studied. Note that this problem cannot be solved by real SUSY-breaking parameters, because the CP phases of off-diagonal elements of sfermion mass matrices come from the complex Yukawa couplings which are usually assumed to obtain nonvanishing KM phase. We call this (chromo) EDM problem new SUSY CP problem in this paper.

In this paper, we focus on the new SUSY CP problem in the models with natural SUSY spectrum. One easy solution is to take large stop mass although large stop mass destabilizes the weak scale. Another one is to take diagonal up-type Yukawa matrix and therefore, diagonalizing matrix of up-type quark becomes unit matrix, although it is not so easy to obtain it in natural way. One more interesting

solution to this new SUSY CP problem is to take real up-type Yukawa couplings to suppress the (chromo) EDM and complex down-type Yukawa couplings to obtain the KM phase. That possibility has been proposed and discussed in the E_6 GUT with family and CP symmetry[15,20], which is spontaneously broken by a CP phase in Higgs vacuum expectation value (VEV) which breaks the family symmetry also.

In this paper, we calculate the chromo EDMs (CEDMs) of up and down quarks in the MSSM with different boundary conditions because the CEDMs give more severe constraints than the usual EDMs for natural SUSY-type models with real SUSY-breaking parameters. (In the recent paper [21], the EDM constraints in natural SUSY models with complex SUSY-breaking parameters has been discussed. However, the contributions discussed in this paper often give stronger constraints to the natural SUSY-type models even if SUSY-breaking parameters are real.) We also discuss the decoupling features of those constraints. First, we show that the nondecoupling feature of the up-quark CEDM contribution by the MIA and that the stop mass must be larger than 10 TeV to satisfy the CEDM constraints. Second, we calculate the up- and down-quark CEDMs numerically in the MSSM and show that the stop mass and the other squark masses must be larger than 7 TeV to satisfy the up- and down-quark CEDMs. If the real up-type Yukawa couplings are adopted, CEDM constraints can be satisfied even if the stop mass is $O(1)$ TeV, although the other squark masses must be larger than 7 TeV. Finally, we discuss the predictions.

II. ROUGH ESTIMATE OF CEDM

In this section, we calculate CEDM of up quark in the modified universal sfermion mass spectrum by MIA, and see the nondecoupling feature in the limit $m_0 \to \infty$ when m_3 and the other SUSY-breaking parameters are fixed.

The effective lagrangian for CEDM is described as

$$\mathcal{L}_{\rm CEDM} = -\frac{ig_s}{2} d_q^C \bar{q}(G\cdot\sigma)\gamma_5 q, \tag{7}$$

where g_s is the QCD coupling, $G\cdot\sigma = G^A_{\mu\nu}T^A\sigma^{\mu\nu}$, $G^A_{\mu\nu}$ is field strength of gluon, T^A $(A=1,2,\ldots,8)$ are $SU(3)$ generators and $\sigma^{\mu\nu} = \frac{i}{2}[\gamma^\mu,\gamma^\nu]$. d_q^C shows quark CEDM and one can calculate this by computing diagrams shown in Fig. 1(a). In particular, d_q^C is dominated by gluino contributions in the SUSY model. In the natural SUSY-type models, the diagram in Fig. 1(b) dominantly contributes to d_u^C[14,15]. We estimate the magnitude of d_u^C by using the diagram in Fig. 1(b) by MIA as

$$\begin{aligned} d_u^C &\simeq \frac{\alpha_s}{4\pi} F\left(\frac{M_{\tilde{g}}^2}{m_{\tilde{u}}^2}, \frac{m_{\tilde{t}}^2}{m_{\tilde{u}}^2}\right) {\rm Im}\left[\frac{M_{\tilde{g}}}{m_{\tilde{t}}^2}\frac{(\Delta^u_{RL})_{33}}{m_{\tilde{t}}^2}\frac{(\Delta^u_{LL})_{31}}{m_{\tilde{u}}^2}\frac{(\Delta^u_{RR})_{13}}{m_{\tilde{u}}^2}\right] \\ &\sim \frac{\alpha_s}{4\pi} F\left(\frac{M_{\tilde{g}}^2}{m_{\tilde{u}}^2}, \frac{m_{\tilde{t}}^2}{m_{\tilde{u}}^2}\right) \frac{M_{\tilde{g}} A_{u33} v_u}{m_{\tilde{t}}^4} {\rm Im}[(\delta^u_{LL})_{31}(\delta^u_{RR})_{13}], \end{aligned} \tag{8}$$

where $(\delta^u_{AB})_{ij}$ are the mass insertion parameters, defined as

$$(\delta^u_{AB})_{ij} \equiv \frac{(\Delta^u_{AB})_{ij}}{m_{\tilde{u}}^2}, \qquad (A,B = L \text{ or } R, i,j = 1,2,3), \tag{9}$$

and $F(x,y)$ is a loop function. In this definition, $(\Delta^u_{AB})_{ij}$ is an element of the 6×6 sfermion mass matrix in the super-CKM basis,

$$\begin{aligned} M_{\tilde{u}}^2 &= \begin{pmatrix} L_u^\dagger(m_Q^2 + v_u^2 Y_u^* Y_u^T)L_u & L_u^\dagger(v_u A_u^* - \mu v_d Y_u^*)R_u^* \\ R_u^T(v_u A_u^T - \mu v_d Y_u^T)L_u & R_u^T(m_u^2 + v_u^2 Y_u^T Y_u^*)R_u^* \end{pmatrix} \\ &\equiv \begin{pmatrix} (\Delta^u_{LL}) & (\Delta^u_{LR}) \\ (\Delta^u_{RL}) & (\Delta^u_{RR}) \end{pmatrix}, \end{aligned} \tag{10}$$

where A_u is a 3×3 matrix for scalar three point vertex, m_Q^2 and m_u^2 are 3×3 soft SUSY-breaking mass matrices, and v_u and v_d are MSSM Higgs VEVs. Here, L_u, R_u are diagonalizing matrices for Yukawa coupling Y_u as $L_u^T Y_u R_u = \hat{Y}_u$ which is a diagonal matrix of Y_u. In the last similarity in Eq. (8), we have assumed that the gluino

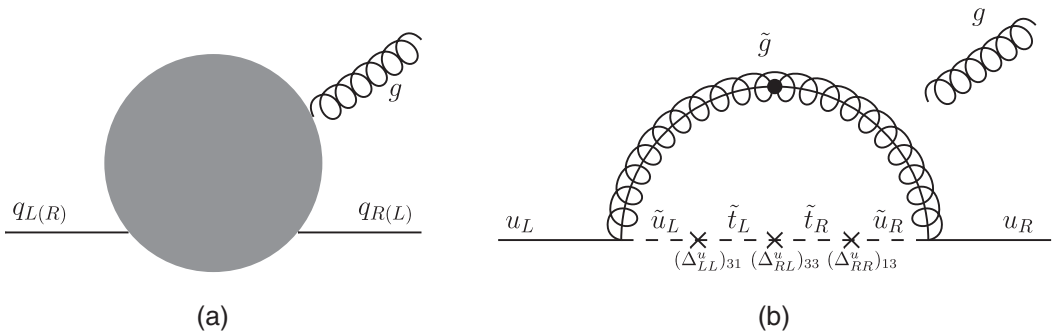

FIG. 1. Diagrams contribute to d_q^C (a) and d_u^C (b). $(\Delta^u_{AB})_{ij}(A,B = L \text{ or } R, i,j = 1,2,3)$ is the element of 6×6 sfermion mass matrix [see Eq. (10)].

mass $M_{\tilde{g}}$ and $(\Delta^u_{RL})_{33} \sim A_{u33} v_u$ are real. Even if all SUSY-breaking parameters and Higgsino mass μ are set to be real, $M^2_{\tilde{u}}$ becomes complex generically because Yukawa couplings are taken to be complex to obtain the KM phase and therefore diagonalizing matrices L_u and R_u are complex. Quantitative constraint for mass insertion parameter in Eq. (8) comes from the current CEDM bound, $|d^C_u| < 3.4 \times 10^{-27} (1.0 \times 10^{-25})$ cm, which are obtained from the present upper limit of $d_{\rm Hg}(d_{\rm N})$ in Eq. (5) [in Eq. (4)], and the relation $d_{\rm Hg} \sim 2.2 \times 10^{-3} e (d^C_u - d^C_d)$[18].[1] ($d_{\rm N} \sim -0.3 e (d^C_u - d^C_d)$[17]), as

$$\mathrm{Im}[(\delta^u_{LL})_{31} (\delta^u_{RR})_{13}] < \left\{ \begin{array}{l} 5.3 \times 10^{-6} (\mathrm{Hg}) \\ 1.6 \times 10^{-4} (\mathrm{neutron}) \end{array} \right\} \left(\frac{m_{\tilde{t}}}{2\ \mathrm{TeV}} \right)^2, \tag{11}$$

where we have used $g_s \simeq 1$, $m_{\tilde{t}} \sim A_{u33} \sim 2$ TeV, $M_{\tilde{g}} \sim 1.5 m_{\tilde{t}} \sim 3$ TeV,[2] $m_{\tilde{u}} \sim 10$ TeV, and the loop integral function $F(0.09, 0.04)$ is 0.079 which is obtained from the Appendix. When we assume that

$$L_u, R_u \sim V_{\rm CKM} \sim \begin{pmatrix} 1 & \lambda & \lambda^3 \\ \lambda & 1 & \lambda^2 \\ \lambda^3 & \lambda^2 & 1 \end{pmatrix} \tag{12}$$

and $m_{\tilde{u}} = m_{\tilde{c}} \gg m_{\tilde{t}}$, the left-hand side of Eq. (11) becomes

$$\mathrm{Im}[(\delta^u_{LL})_{31} (\delta^u_{RR})_{13}] \simeq \left(\frac{m^2_{\tilde{t}} - m^2_{\tilde{u}}}{m^2_{\tilde{u}}} \right)^2 \times \lambda^6 \quad (\lambda = 0.22). \tag{13}$$

So this contribution does not decouple in the limit of $m_{\tilde{u}} \to \infty$ and the size is about 10^{-4} that is about 20 times larger than the constraint from Hg EDM. Therefore, $m_{\tilde{t}} > 10$ TeV is required to satisfy the CEDM constraint in this approximation.

On the other hand, for the CEDM of down quark, d^C_d, such contributions from flavor-violating mass insertion is decoupled when sdown mass $m_{\tilde{d}} \to \infty$ because the right-handed sbottom mass $m_{\tilde{b}} \sim m_{\tilde{d}}$. Therefore, $m_{\tilde{d}} > 10$ TeV is expected to be required to satisfy the experimental bound of CEDM if the decoupling feature is similar to that of d^C_u for $m_{\tilde{t}}$.

[1]Here, we use the bound for $|d^C_u - d^C_d|$ as the bound for d^C_u. This is justified in the limit $m_0 \to \infty$ because d^C_d is vanishing in the limit. In this paper, we just use the bound for $d^C_u - d^C_d$ as the bound for d^C_u and d^C_d even with finite m_0.

[2]If A-term is smaller, the constraints become weaker, although $A \ll M_{\tilde{g}}$ usually requires a tuning in the MSSM with SUSY-breaking parameters given at the GUT scale because of the renormalization group effects.

Therefore, the CEDM of up quark is more serious in natural SUSY scenario. One simple solution is that real Y_u and A_u are taken while Y_d is complex that induces the KM phase. In this case, diagonalizing matrices of up-type quark mass matrix are also real and then d^C_u is strongly suppressed. Note that Y_u becomes complex through the renormalization group equation (RGE), even if Y_u is real at the GUT scale. In such a case, however, d^C_u is small enough to satisfy the current experimental bound as we will show in Sec. III.

III. EVALUATIONS AND RESULTS

In this section, we numerically calculate the CEDM in the MSSM with the modified universal sfermion mass spectrum.

Now, we explain the procedure for the calculation of CEDMs. First of all, input parameters, which are gauge couplings g_i, gaugino masses M_i, Yukawa couplings, A parameters which are couplings of three scalar's vertex, sfermion mass matrices, and doublet Higgs masses are given at the GUT scale, $\Lambda_{\rm G} = 2 \times 10^{16}$ GeV, as

$$g_1(\Lambda_{\rm G}) = g_2(\Lambda_{\rm G}) = g_3(\Lambda_{\rm G}) = g_{\rm GUT} = 0.7, \tag{14}$$

$$M_1(\Lambda_{\rm G}) = M_2(\Lambda_{\rm G}) = M_3(\Lambda_{\rm G}) = M_{1/2}, \tag{15}$$

$$Y_u \sim \begin{pmatrix} \lambda^6 & \lambda^5 & \lambda^3 \\ \lambda^5 & \lambda^4 & \lambda^2 \\ \lambda^3 & \lambda^2 & 1 \end{pmatrix}, \quad A_u \sim A_0 \begin{pmatrix} \lambda^6 & \lambda^5 & \lambda^3 \\ \lambda^5 & \lambda^4 & \lambda^2 \\ \lambda^3 & \lambda^2 & 1 \end{pmatrix}, \tag{16}$$

$$Y_d \sim Y^T_e \sim \begin{pmatrix} \lambda^6 & \lambda^{5.5} & \lambda^5 \\ \lambda^5 & \lambda^{4.5} & \lambda^4 \\ \lambda^3 & \lambda^{2.5} & \lambda^2 \end{pmatrix},$$

$$A_d \sim A^T_e \sim A_0 \begin{pmatrix} \lambda^6 & \lambda^{5.5} & \lambda^5 \\ \lambda^5 & \lambda^{4.5} & \lambda^4 \\ \lambda^3 & \lambda^{2.5} & \lambda^2 \end{pmatrix}, \tag{17}$$

$$\tilde{m}^2_{\mathbf{10}} = \begin{pmatrix} m^2_0 & 0 & 0 \\ 0 & m^2_0 & 0 \\ 0 & 0 & m^2_3 \end{pmatrix}, \qquad \tilde{m}^2_{\bar{\mathbf{5}}} = \begin{pmatrix} m^2_0 & 0 & 0 \\ 0 & m^2_0 & 0 \\ 0 & 0 & m^2_0 \end{pmatrix}, \tag{18}$$

$$m^2_{H_u}(\Lambda_{\rm G}) = m^2_{H_d}(\Lambda_{\rm G}) = (500\ \mathrm{GeV})^2, \tag{19}$$

where A_0 is the typical scale of A parameters, and sfermion mass matrices $\tilde{m}^2_{\mathbf{10}}$ and $\tilde{m}^2_{\bar{\mathbf{5}}}$ are for $\mathbf{10}$ and $\bar{\mathbf{5}}$ fields, respectively. The Higgsino mass μ is fixed by the value of the Z boson mass m_Z. (μ becomes comparatively large ($O(1)$ TeV), which may destabilize the weak scale. But we do not mind it because large μ does not contribute much to d^C_u.) Next, in order to obtain low-energy parameters from

these inputs, we use two-loop RGEs based on Ref. [22]. Note that, for simplicity, we consider MSSM from GUT scale to the SUSY-breaking scale. Finally, we compute up, down and strange quark CEDMs. These CEDMs denoted as d_q^C $(q = u, d, s)$ are evaluated by the following one-loop formulas,

$$d_u^C = c\frac{\alpha_s}{4\pi}\sum_{j=1}^{6}\frac{M_{\tilde{g}}}{(\hat{M}^2_{\tilde{u}})_{jj}} \times\left\{\left(-\frac{1}{3}F_1(x_j^u)-3F_2(x_j^u)\right)\mathrm{Im}[(U^\dagger_{\tilde{u}})_{1j}(U_{\tilde{u}})_{j4}]\right\}, \quad (20)$$

$$d_d^C = c\frac{\alpha_s}{4\pi}\sum_{j=1}^{6}\frac{M_{\tilde{g}}}{(\hat{M}^2_{\tilde{d}})_{jj}} \times\left\{\left(-\frac{1}{3}F_1(x_j^d)-3F_2(x_j^d)\right)\mathrm{Im}[(U^\dagger_{\tilde{d}})_{1j}(U_{\tilde{d}})_{j4}]\right\}, \quad (21)$$

$$d_s^C = c\frac{\alpha_s}{4\pi}\sum_{j=1}^{6}\frac{M_{\tilde{g}}}{(\hat{M}^2_{\tilde{d}})_{jj}} \times\left\{\left(-\frac{1}{3}F_1(x_j^d)-3F_2(x_j^d)\right)\mathrm{Im}[(U^\dagger_{\tilde{d}})_{2j}(U_{\tilde{d}})_{j5}]\right\}, \quad (22)$$

where $c \sim 0.9$ is QCD correction. $\hat{M}^2_{\tilde{q}}$ $(q = u, d)$ are diagonalized squark mass matrices which are obtained as $\hat{M}^2_{\tilde{q}} = U_{\tilde{q}} M^2_{\tilde{q}} U^\dagger_{\tilde{q}}$, where $M^2_{\tilde{q}}$ and $U_{\tilde{q}}$ are 6×6 squark mass matrices and the diagonalizing matrices, respectively. $F_1(x) = (x^2 - 4x + 3 + 2\ln x)/2(1-x)^3$ and $F_2(x) = (x^2 - 1 - 2x\ln x)/2(1-x)^3$ are coming from loop integrals and $x_j^q = \frac{M^2_{\tilde{g}}}{(\hat{M}^2_{\tilde{q}})_{jj}}$. The current bounds [13,14] are

$$|d_q^C| < 3.4\times 10^{-27}\ \text{cm} \quad (q = u, d), (\text{Hg}) \quad (23)$$

$$|d_q^C| < 1.0\times 10^{-25}\ \text{cm} \quad (q = u, d), (\text{neutron}) \quad (24)$$

$$|d_s^C| < 1.1\times 10^{-25}\ \text{cm}. \quad (25)$$

We consider three types of inputs of Yukawa couplings and A parameters. All of three types have the hierarchy explained above, but have different type of $\mathcal{O}(1)$ coefficients. To explain this, we show the explicit forms of these matrices:

$$Y_u = \begin{pmatrix} y_{u11}\lambda^6 & y_{u12}\lambda^5 & y_{u13}\lambda^3 \\ y_{u21}\lambda^5 & y_{u22}\lambda^4 & y_{u23}\lambda^2 \\ y_{u31}\lambda^3 & y_{u32}\lambda^2 & y_{u33} \end{pmatrix},$$
$$A_u = A_0\begin{pmatrix} a_{u11}\lambda^6 & a_{u12}\lambda^5 & a_{u13}\lambda^3 \\ a_{u21}\lambda^5 & a_{u22}\lambda^4 & a_{u23}\lambda^2 \\ a_{u31}\lambda^3 & a_{u32}\lambda^2 & 1 \end{pmatrix}, \quad (26)$$

$$Y_d = \begin{pmatrix} y_{d11}\lambda^6 & y_{d12}\lambda^{5.5} & y_{d13}\lambda^5 \\ y_{d21}\lambda^5 & y_{d22}\lambda^{4.5} & y_{d23}\lambda^4 \\ y_{d31}\lambda^3 & y_{d32}\lambda^{2.5} & y_{d33}\lambda^2 \end{pmatrix},$$
$$A_d = A_0\begin{pmatrix} a_{d11}\lambda^6 & a_{d12}\lambda^{5.5} & a_{d13}\lambda^5 \\ a_{d21}\lambda^5 & a_{d22}\lambda^{4.5} & a_{d23}\lambda^4 \\ a_{d31}\lambda^3 & a_{d32}\lambda^{2.5} & a_{d33}\lambda^2 \end{pmatrix}, \quad (27)$$

$$Y_e = \begin{pmatrix} y_{e11}\lambda^6 & y_{e12}\lambda^5 & y_{e13}\lambda^3 \\ y_{e21}\lambda^{5.5} & y_{e22}\lambda^{4.5} & y_{e23}\lambda^{2.5} \\ y_{e31}\lambda^5 & y_{e32}\lambda^4 & y_{e33}\lambda^2 \end{pmatrix},$$
$$A_e = A_0\begin{pmatrix} a_{e11}\lambda^6 & a_{e12}\lambda^5 & a_{e13}\lambda^3 \\ a_{e21}\lambda^{5.5} & a_{e22}\lambda^{4.5} & a_{e23}\lambda^{2.5} \\ a_{e31}\lambda^5 & a_{e32}\lambda^4 & a_{e33}\lambda^2 \end{pmatrix}. \quad (28)$$

(i) *real Y_u type*
At the GUT scale, y_{dij}, a_{dij}, y_{eij} and a_{eij} are complex $\mathcal{O}(1)$ coefficients, while y_{uij} and a_{uij} are real $\mathcal{O}(1)$ coefficients (i, $j = 1, 2, 3$).

(ii) *complex Y_u type*
All y_{uij}, a_{uij}, y_{dij}, a_{dij}, y_{eij} and a_{eij} are complex $\mathcal{O}(1)$ coefficients (i, $j = 1, 2, 3$).

(iii) *E_6 model* (with family symmetry and spontaneous CP violation) There are special relations obtained in the model in Ref. [20]: $y_{u11} = y_{u13} = y_{u31} = y_{e13} = y_{e21} = 0$, $y_{u12} = -y_{u21} = y_{d13} = \frac{1}{3}d_q$, $y_{u23} = y_{u32}$, $y_{d23} = y_{e32}$, $y_{d33} = y_{e33}$ and $y_{e12} = -y_{e31}$. y_{d11}, y_{d12}, y_{d22}, y_{d32}, y_{e11}, y_{e22} and y_{e23} are complex $\mathcal{O}(1)$ coefficients, and d_q, y_{u22}, y_{u23}, y_{u33}, y_{d21}, y_{d23}, y_{d31}, y_{d33} and y_{e12} are real $\mathcal{O}(1)$ coefficients (there are same structures in A parameters).

For all types, we take real parameters for $M_{1/2}$, μ, $A_{u33} = A_0$, and $y_{u33} = 0.8$ at the GUT scale and we set $\tan\beta = 7$. In these parameters, most of the usual contributions to EDMs are strongly suppressed especially when $m_0 \to \infty$. We take A parameters which have similar hierarchies to the corresponding Yukawa couplings. This situation can be realized in models in which hierarchies of Yukawa couplings are explained by the Froggatt-Nielsen mechanism[23]. In such situation, we think it reasonable that $O(1)$ coefficients of A parameters are complex number when the $O(1)$ coefficients of corresponding Yukawa couplings are complex as in Ref. [6,15,20]. We checked that the numerical results do not change at all if all $O(1)$ coefficients of A parameters are taken to be real for all types above.

We need to make a few comments on $\mathcal{O}(1)$ coefficient. The complex $\mathcal{O}(1)$ coefficient C means that $C = |C|\exp(i\theta^{(C)})$ as $|C|$ is real $\mathcal{O}(1)$ coefficient and $\theta^{(C)}$ is random number in the ranges $0 \le \theta^{(C)} \le 2\pi$. In addition,

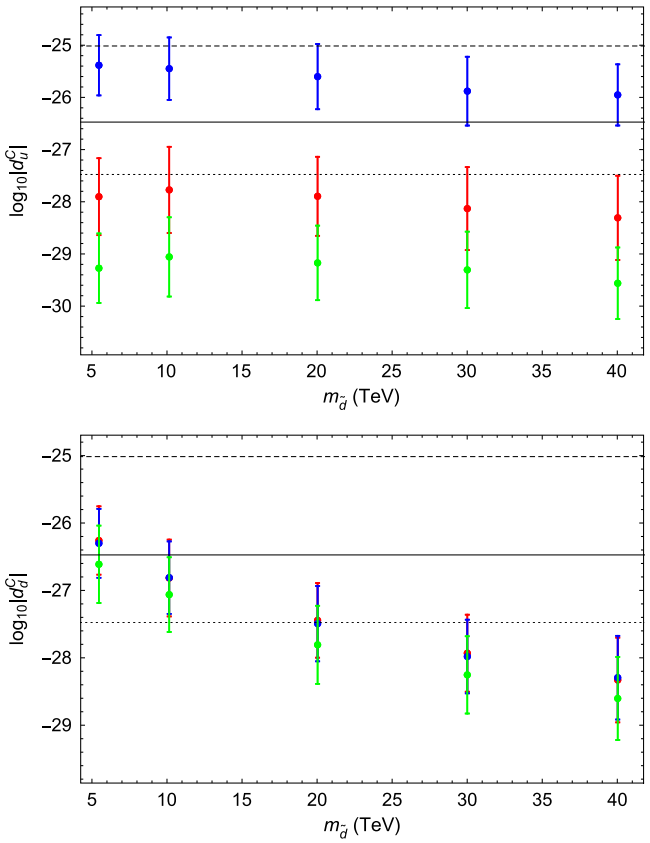

FIG. 2. $m_{\tilde{q}}$ dependence of d_u^C (upper panel) and d_d^C (lower panel). Red, Blue and Green plots are *real* Y_u *type*, *complex* Y_u *type* and E_6 *model*, respectively. Each error bar shows the standard deviation for the predicted values of $\log_{10}|d_q^C|$ $(q = u, d)$ which are obtained in various model points with different $O(1)$ coefficients. The black solid line is the current bound from Hg EDM and the allowed region is the lower area. The dashed line shows the current bound from the neutron EDM, and the dotted line is the bound expected in future experiments of neutron EDM. We choose m_3 and $M_{1/2}$ to become light stop at the SUSY scale (1 TeV), and in these figures, we set $m_{\tilde{t}} = (2000 \pm 250)$ GeV. We also set $A_0 = -1$ TeV.

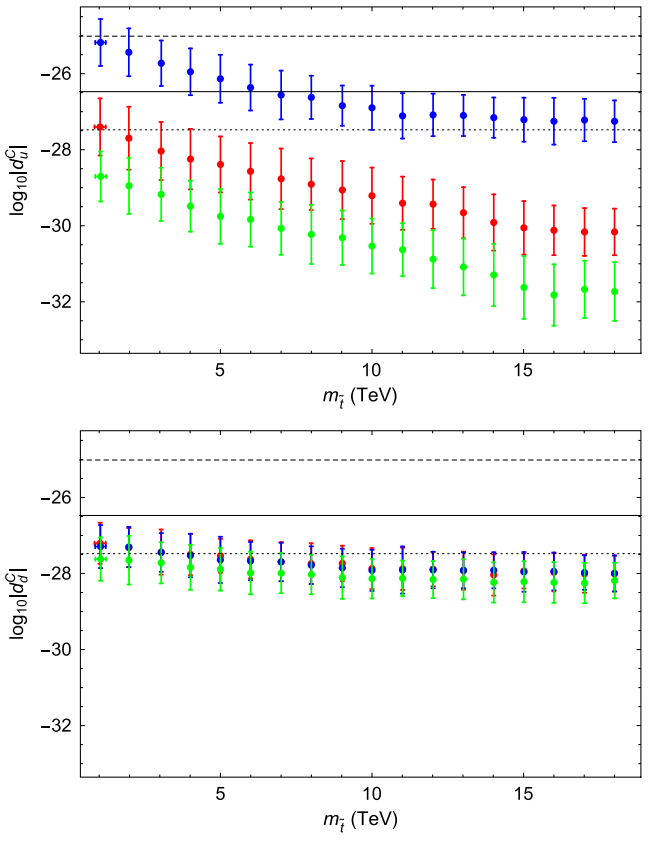

FIG. 3. $m_{\tilde{t}}$ dependence of d_u^C (upper panel) and d_d^C (lower panel). The red, blue, and green plots are *real* Y_u *type*, *complex* Y_u *type*, and the E_6 *model*, respectively. Each vertical error bar shows the standard deviation for the predicted values of $\log_{10}|d_q^C|$ $(q = u, d)$ which are obtained in various model points with different $O(1)$ coefficients. The horizontal error bar shows the distribution of stop masses by variation of $O(1)$ coefficients of Yukawa couplings and A parameters. The black solid line is current bound from Hg EDM and allowed region is lower area. The dashed line shows the current bound from neutron EDM, and the dotted line is the bound expected in future experiments of neutron EDM. In these figures, we set $m_0 = 10$ TeV and $A_0 = -1$ TeV.

real $\mathcal{O}(1)$ coefficient means random number within the interval 0.5 to 1.5 with $+$ or $-$ signs[3]

We have calculated CEDMs in $O(100)$ model points with different $O(1)$ coefficients and obtained the average and the standard deviation of $\log_{10}|d_q^C|$ which are shown in Figs. 2–5 as the center value and the error bar, respectively. For simplicity, we do not impose the conditions to obtain realistic CKM matrix in our calculation. The result is below. First we show $m_0(m_{\tilde{q}})$ dependence of CEDMs in Fig. 2. The vertical axis is $\log_{10}|d_u^C|$ (upper panel) and $\log_{10}|d_d^C|$ (lower panel), and the horizontal axis is heavy sfermion mass at low energy denoted as $m_{\tilde{q}}$, which is almost determined by m_0 value. Red, blue and green plots are *real* Y_u *type*, *complex* Y_u *type* and E_6 *model*, respectively. Black solid line is current bound from Hg EDM and allowed region is lower area. Dashed line shows the current bound from neutron EDM, and the dotted line is the bound expected in future experiments of neutron EDM [24]. We set $A_0 = -1$ TeV at the GUT scale. In these figures, we choose $M_{1/2}$ and m_3 so that stop mass at the SUSY scale[4] become about 2 TeV in each m_0 case, and $M_{\tilde{g}}$ and $|A_{u33}|$

[3]We don't contain one-loop threshold corrections in the calculation because $\mathcal{O}(1)$ coefficients produce a much greater difference in the results of CEDM than the threshold correction, although we should take into account the one-loop threshold corrections when we consider two-loop RGEs.

[4]In this paper, we take the SUSY scale $= 1$ TeV as the renormalization scale, even when the squark masses are much larger than 1 TeV.

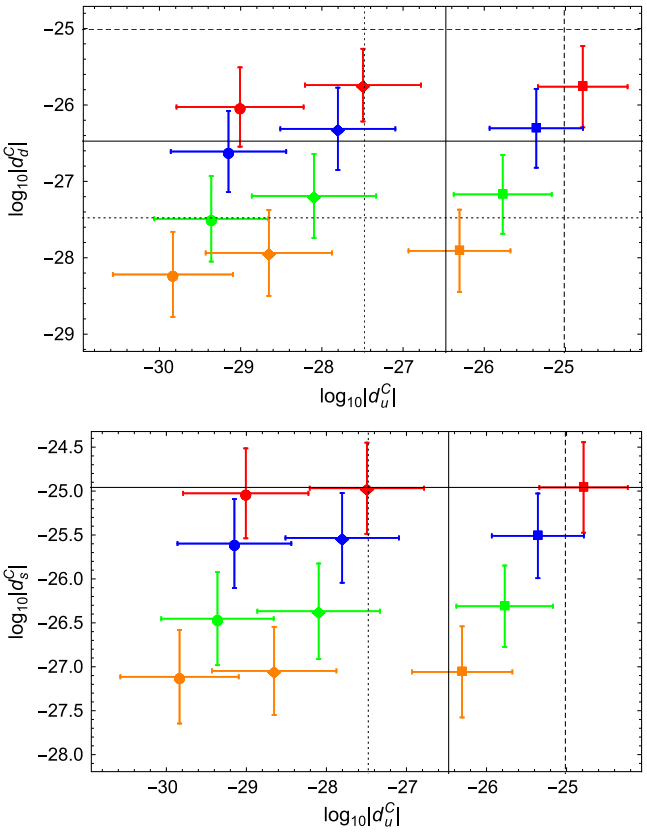

FIG. 4. Up, down and strange quark CEDM in three type of boundary condition of Y_u. Upper panel is up and down quark CEDM and lower panel is up and strange quark CEDM. Diamond, square and circle plots are *real* Y_u *type*, *complex* Y_u *type* and E_6 *model*, respectively. Red, blue, green and orange mean that m_0 is 5 TeV, 10 TeV, 20 TeV and 40 TeV. Each error bar shows the standard deviation for the predicted values of $\log_{10}|d_q^C|$ $(q = u, d, s)$ which are obtained in various model points with different $O(1)$ coefficients. Black solid line is the current bound from Hg EDM and allowed region is lower left area. Dashed line shows the current bound from neutron EDM, and the dotted line is the bound expected in future experiments of neutron EDM.

value at the SUSY scale is shown in Table I. From Fig. 2, it is clear that d_d^C is decoupled when m_0 increases and we found that roughly $m_{\tilde{d}} > 7$ TeV is required to satisfy the current bound from Hg EDM, corresponding to the situation setting $m_0 > 7$ TeV at GUT scale. (In this paper, we discuss the limit of sfermion masses by using the center value in the distribution.) However, because of nondecoupling effect caused by stop contribution, current bound for d_u^C is severe if Y_u is complex at GUT scale. In order to satisfy the current bound in the *complex* Y_u *type*, $m_{\tilde{t}}$ must be larger.

How large $m_{\tilde{t}}$ is required to suppress d_u^C sufficiently? We show $m_{\tilde{t}}$ dependence of CEDMs in Fig. 3. The vertical axis is $\log_{10}|d_u^C|$ (upper panel) and $\log_{10}|d_d^C|$ (lower panel), and the horizontal axis is $m_{\tilde{t}}$. The colors of plots and shapes of

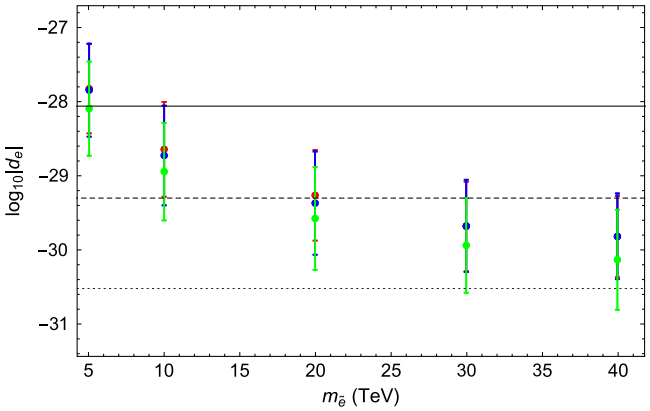

FIG. 5. $m_{\tilde{e}}$ dependence of d_e in three type of boundary condition of Y_u. Red, Blue and Green plots are *real* Y_u *type*, *complex* Y_u *type* and E_6 *model*, respectively. Each error bar shows the standard deviation for the predicted values of $\log_{10}|d_e|$ which are obtained in various model points with different $O(1)$ coefficients. Black solid line is current bound and allowed region is the lower area. Other input parameters are same as for the Fig. 2. The dashed(dotted) line shows the future bound expected by ACME II (III)[28].

lines have the same meanings as in Fig. 2. In these figures, we set $m_0 = 20$ TeV and $A_0 = -1$ TeV at GUT scale. $M_{\tilde{g}} = 3$ TeV and $m_{\tilde{t}} \equiv \sqrt{m_{\tilde{t}1} m_{\tilde{t}2}}$ are given at the SUSY scale, where $m_{\tilde{t}_1}^2$ and $m_{\tilde{t}_2}^2$ are eigenvalues of the matrix of

TABLE I. $M_{\tilde{g}}$ and $|A_{u33}|$ at the SUSY scale (1 TeV) in each m_0 value for calculation in Fig. 2.

m_0 (TeV)	$M_{\tilde{g}}$ (TeV)	$\lvert A_{u33}\rvert$ (TeV)
5	2.7	2.0
10	2.8	2.1
20	4.3	3.1
30	6.2	4.4
40	8.4	5.8

TABLE II. GUT scale parameters which we use in each m_0 value.

m_0 (TeV)	m_3 (TeV)	$M_{1/2}$ (TeV)	A_0 (TeV)
5	1.2	1.5	−5 TeV
10	1.5	1.8	−4.5 TeV
20	2	2.4	−2.5 TeV
40	3.5	4.5	−3.5 TeV

TABLE III. $m_{\tilde{t}}$ and $|A_{u33}|$ at SUSY scale in each m_0 value.

m_0 (TeV)	$m_{\tilde{t}}$ (TeV)	$\lvert A_{u33}\rvert$ (TeV)
5	1.9	3.4
10	2.3	3.7
20	2.6	4.1
40	4.3	7.4

TABLE IV. Neutralino masses at SUSY scale in each m_0 case. In this calculation, the masses of two heavy neutralinos, m_{N_3} and m_{N_4}, are almost degenerated.

m_0 (TeV)	m_{N_1} (TeV)	m_{N_2} (TeV)	m_{N_3}, m_{N_4} (TeV)
5	0.5	0.9	2.1
10	0.6	1.0	2.4
20	0.8	1.5	3.3
30	1.2	2.2	4.2
40	1.6	3.0	5.2

stop mass square. Then $A_{u33} \sim 2.2$ TeV at the SUSY scale. From Fig. 3, it is easy to understand that d_u^C is strongly dependent on $m_{\tilde{t}}$, while d_d^C is almost independent. The flat regions appear also in d_u^C, which are caused by the contributions from the first two generation squarks. Roughly, when $m_{\tilde{t}} > 7$ TeV, current bound of d_u^C from Hg EDM is satisfied even if Y_u is complex at GUT scale. (Note that this lower limit for $m_{\tilde{t}}$ is not so far from the prediction obtained by the MIA as well as the lower limit for $m_{\tilde{d}}$.) However, from the point of view of naturalness, it is preferable that $m_{\tilde{t}}$ has smaller value, so such a large stop mass may not be acceptable. *real Y_u type* and E_6 *model* are satisfying d_u^C bound even if the stop mass is smaller than 1 TeV. Therefore, real Y_u at GUT scale can be an important condition to satisfy d_u^C bound when $m_{\tilde{t}} \sim \mathcal{O}(1)$ TeV.

We have investigated $m_{\tilde{d}}$ or $m_{\tilde{t}}$ dependence of strange quark CEDM d_s^C. The results are very similar to d_d^C results and constraints of d_s^C are much weaker than that of d_d^C (see Fig. 4.), and therefore, we do not discuss the strange quark CEDM in detail in this paper.

Finally, we check whether 125 GeV Higgs mass is really obtained in our setup. To do this, we use `FeynHiggs-2.10` [25]. We set GUT scale parameters as shown in Table II. $M_{1/2}$, m_3, and A_0 are chosen so that all sfermions have positive squared masses at SUSY scale. We also show $m_{\tilde{t}}$ and $|A_{u33}|$ at SUSY scale in Table III. We found that the 125 GeV Higgs mass is realized in all three types. The values of CEDMs in each situation are shown in Fig. 4. Upper panel is d_u^C versus d_d^C, and lower panel is d_u^C versus d_s^C. In these figures, diamond, square and circle plots are corresponding to *real Y_u type*, *complex Y_u type* and E_6 *model*, respectively. Red, blue, green and orange means that m_0 is 5 TeV, 10 TeV, 20 TeV and 40 TeV. Each error bar shows the standard deviation for the predicted values of $\log_{10}|d_q^C|$ $(q = u, d, s)$ which are obtained in various model points with different $O(1)$ coefficients. Black solid line is current bound from Hg EDM and allowed region is lower left area. Dashed line shows the current bound from neutron EDM, and the dotted line is the bound expected in future experiments of neutron EDM. From Fig. 4, it is clear that d_u^C bound for *complex Y_u type* is severe, even when 125 GeV Higgs mass is realized. In E_6 *model*, each CEDM value is smaller than that of the other two types because of the special structures of Y_u and A_u at the GUT scale. Therefore, these structures have some effects to suppress $|d_u^C|$ value.

IV. COMMENT ON ELECTRON EDM

Recently, the constraint of electron EDM, d_e, is improved [26] and may be severe for this discussion. Then we also check the constraint of d_e in the same situations discussed above. Note that we evaluate d_e by using the expression based on Ref. [27]. Although there are mainly two types of contributions to d_e in SUSY model, neutralino and chargino contributions, we ignore the chargino contributions because Higgsinos are heavier than wino. So, we will show the d_e result for the sum of four neutralino contributions in our setup.

The result is shown in Fig. 5. The vertical axis is $\log_{10}|d_e|$. In this case, we set horizontal axis as slepton mass at low energy, which is almost determined by m_0 value. Red, blue and green plots are the real Y_u type, complex Y_u type, and E_6 model, respectively. Black solid line is current bound, $|d_e| < 8.7 \times 10^{-29}$ e cm [26], and allowed region is lower area. Other input parameters which are used for calculation are the same as for the Fig. 2. Neutralino masses at SUSY scale in each m_0 case are shown in Table IV.

Compared with Figs. 2 and 5, we found that constraint of d_e is weaker than that of d_d^C at least in the situation we discussed in this paper. Roughly speaking, $m_{\tilde{e}} > 6$ or 7 TeV is required for the d_e bound in real Y_u type and complex Y_u type while d_e bound is still satisfied with $m_{\tilde{e}} > 5$ TeV in the E_6 model. This is because there are special structures not only for Y_u and Y_d but also for the Y_e in the E_6 model. Electron EDM experiments will be improved in a few years [28], so we should care about not only the CEDM bounds but also this bound. The expected future bounds are presented in Fig. 5. Interestingly, we can expect a signal of the electron EDM in the future. If it is not seen, m_0 must be larger than 40 TeV.

V. SUMMARY AND DISCUSSION

In this paper, we discussed the CEDM bounds in the SUSY model with the natural SUSY-type sfermion mass spectrum in which the stop masses $m_{\tilde{t}}$ are $O(1)$ TeV while the other squark masses m_0 are much larger than $m_{\tilde{t}}$ since the CEDM constraints, especially from the Hg EDM, give severe constraints to this natural SUSY-type sfermion mass spectrum even if real SUSY-breaking parameters are assumed. We calculated the CEDM of up, down, and strange quarks numerically at the three boundary conditions for Yukawa couplings at the GUT scale, the real Y_u type, complex Y_u type, and the E_6 model, and discussed

their decoupling features. First, we concluded that the up-quark CEDM becomes sufficiently small to satisfy the experimental bound when up-quark Yukawa couplings are real at the GUT scale even if we take $m_{\tilde{t}} \sim O(1)$ TeV not to destabilize the weak scale, while it becomes too large when the Yukawa couplings are complex even if $m_0 \gg m_{\tilde{t}}$. On the other hand, the down and strange quark CEDM become sufficiently small if $m_0 > 7$ TeV because of the decoupling feature. Second, to satisfy the up-quark CEDM constraint with complex Y_u, $m_{\tilde{t}} > 7$ TeV is needed, which destabilizes the weak scale.

In the natural SUSY-type sfermion mass spectrum, off-diagonal elements of (Δ^d_{RR}), which is defined as the same rule in Eq. (10), are strongly suppressed because the masses of the right-handed sdown type are almost degenerated. For this reason, a dominant contribution to d^C_d is proportional to $\mathrm{Im}[(\Delta^d_{LL})_{31}(\Delta^d_{RL})_{13}]$ ($\propto A_{d13}$ in the super-CKM basis) rather than $\mathrm{Im}[(\Delta^d_{LL})_{31}(\Delta^d_{RL})_{33}(\Delta^d_{RR})_{13}]$. When the A parameters are proportional to the corresponding Yukawa couplings $A_f \propto Y_f$ ($f = u$, d, e) at the GUT scale, off-diagonal elements of A parameters in the super-CKM basis are suppressed at the SUSY-breaking scale and, therefore, d^C_d is strongly suppressed ($\sim \mathcal{O}(10^{-32})e$ cm). In such a case, we cannot constrain the sfermion masses from the bound of d^C_d even when the CEDM constraints are improved at the level of the future neutron EDM sensitivity. Note that this situation can be also realized when $A_0 = 0$ at the GUT scale. On the other hand, in the case of $A_f \propto Y_f$ at the GUT scale, d^C_u does not change so much in the natural SUSY-type sfermion mass spectrum because the dominant contribution to d^C_u is proportional to the diagonal element of the A parameter A_{u33} in the super-CKM basis as discussed in Eq. (8). The situation does not change so much in the case of $A_0 = 0$ at the GUT scale since the A_0 value does not affect the value of the diagonal elements of the A parameters at the SUSY-breaking scale so much because of the RGE running. We checked these behaviors numerically, and the lower bounds of $m_{\tilde{t}}$ from the bound of d^C_u are the same as our results.

These constraints are dependent on explicit models for Yukawa couplings and the sfermion mass spectrum. In this paper, we have just demonstrated the constraints from the EDMs in a certain model for the Yukawa couplings and the sfermion mass spectrum, which are obtained from the E_6 GUT with family symmetry. Therefore, the constraints become different from ours if different models for Yukawa couplings are adopted. However, we note that our model will give comparatively weaker constraints than the others because the diagonalizing matrices of the up-type Yukawa matrix have small mixings. (Of course, we can consider the models which give weaker constraints than ours, for example, the diagonal up-type Yukawa matrix model.) Therefore, our constraints to the natural SUSY-type sfermion mass models from d^C_u are quite general.

In this paper, we have neglected the uncertainties in the calculation of the relation between the Hg (neutron) EDM and CEDMs and discussed the constraints. However, the uncertainties for the coefficients are more than 100% for the Hg EDM. Conservatively, we may have to use the constraints only from the neutron EDM. Then, we have almost no constraints from the neutron EDM to the natural SUSY model with $O(1)$ TeV stop mass. In that case, constraints from the electron EDM become important and give lower bounds of m_0, although no constraint for $m_{\tilde{t}}$ is given. Since the experimental sensitivity of the electron EDM is expected to be improved by about 2 orders of magnitude, we can expect that nonvanishing electron EDM is observed in future experiments. If it is not observed, the m_0 is expected to be larger than 40 TeV. To improve the bound for $m_{\tilde{t}}$, future experiments of neutron EDM are important. Since experimental sensitivity of the neutron EDM is expected to be improved by more than two orders of magnitude, the observation of nonvanishing EDM of neutron is expected. No signal means $m_0 > 20$ TeV, and $m_{\tilde{t}} > 20$ TeV if Y_u is complex, while almost no constraint to $m_{\tilde{t}}$ if Y_u is real. One more way to improve the bound for $m_{\tilde{t}}$ is, of course, to reduce the uncertainties in theoretical calculation of Hg EDM.

We conclude that the up quark CEDM constraint can be severe in natural SUSY type sfermion mass spectrum. If experimental bounds of EDM and/or theoretical calculation of Hg EDM are improved in future, they will constrain the lower bounds of stop mass and the other heavy sfermion masses. In addition, if the sfermion masses, especially the stop mass, are observed in future experiments, we may be able to constrain the structure of Y_u at GUT scale by the CEDM constraints.

ACKNOWLEDGMENTS

We thank F. Sala and J. Hisano for advice on the present situation of theoretical calculation of Hg EDM. N. M. is supported in part by Grants-in-Aid for Scientific Research from MEXT of Japan (No. 15K05048). Y. M. is supported in part by the National Research Foundation of Korea (NRF) Research Grant No. NRF-2015R1A2A1A05001869 and the National Natural Science Foundation of China (NSFC) under Contracts No. 11435003, No. 11225523, and No. 11521064. The work of Y. S. is supported by the Japan Society for the Promotion of Science (JSPS) Research Fellowships for Young Scientists, No. 16J08299.

APPENDIX: LOOP INTEGRAL FOR THE DIAGRAM IN FIG. 1(b)

The expression of the up-quark CEDM d^C_u in the mass insertion approximation is

TABLE V. The values of $F_{\rm MIA}(r_{\tilde{g}}, r_{\tilde{t}})$ with several values of $r_{\tilde{g}}$ and $r_{\tilde{t}}$.

$r_{\tilde{t}}\backslash r_{\tilde{g}}$	0.2^2	0.3^2	0.5^2	1^2	2^2	5^2
0.1^2	4.1×10^{-2}	1.1×10^{-2}	1.8×10^{-3}	1.2×10^{-4}	6.9×10^{-6}	1.6×10^{-7}
0.2^2	2.4×10^{-1}	7.9×10^{-2}	1.6×10^{-2}	1.2×10^{-3}	6.9×10^{-5}	1.5×10^{-6}
0.3^2	5.3×10^{-1}	2.0×10^{-1}	4.6×10^{-2}	4.0×10^{-3}	2.4×10^{-4}	5.1×10^{-6}
0.4^2	8.5×10^{-1}	3.6×10^{-1}	9.1×10^{-2}	8.8×10^{-3}	5.6×10^{-4}	1.2×10^{-5}
0.5^2	1.2	5.2×10^{-1}	1.4×10^{-1}	1.5×10^{-2}	1.0×10^{-3}	2.1×10^{-5}
0.6^2	1.4	6.8×10^{-1}	2.0×10^{-1}	2.3×10^{-2}	1.6×10^{-3}	3.4×10^{-5}
0.7^2	1.7	8.2×10^{-1}	2.6×10^{-1}	3.2×10^{-2}	2.3×10^{-3}	5.0×10^{-5}
0.8^2	1.9	9.6×10^{-1}	3.2×10^{-1}	4.1×10^{-2}	3.2×10^{-3}	6.8×10^{-5}
0.9^2	2.1	1.1	3.7×10^{-1}	5.1×10^{-2}	4.1×10^{-3}	8.9×10^{-5}
1^2	2.3	1.2	4.2×10^{-1}	6.1×10^{-2}	5.0×10^{-3}	1.1×10^{-4}
2^2	3.2	1.8	7.6×10^{-1}	1.4×10^{-1}	1.5×10^{-2}	4.0×10^{-4}
5^2	3.7	2.3	1.0	2.4×10^{-1}	3.3×10^{-2}	1.2×10^{-3}

$$d_u^C = \frac{\alpha_s}{4\pi}\frac{M_{\tilde{g}}}{m_{\tilde{t}}^2}\mathrm{Im}[(\delta^u_{LL})_{31}(\delta^u_{RL})_{33}(\delta^u_{RR})_{13}] \times F_{\rm MIA}(r_{\tilde{g}}, r_{\tilde{t}}) \tag{A1}$$

$$F_{\rm MIA}(r_{\tilde{g}}, r_{\tilde{t}}) \equiv 6r_{\tilde{t}}^2\left(-3I_G(r_{\tilde{g}}, r_{\tilde{t}}) + \frac{1}{3}I_{S_1}(r_{\tilde{g}}, r_{\tilde{t}}) + \frac{1}{3}I_{S_2}(r_{\tilde{g}}, r_{\tilde{t}}) + \frac{1}{3}I_{S_3}(r_{\tilde{g}}, r_{\tilde{t}}) + \frac{1}{3}I_{S_4}(r_{\tilde{g}}, r_{\tilde{t}})\right), \tag{A2}$$

where $r_{\tilde{g}} = \frac{M_{\tilde{g}}^2}{m_{\tilde{u}}^2}$, $r_{\tilde{t}} = \frac{m_{\tilde{t}}^2}{m_{\tilde{u}}^2}$ and $I_i(r_{\tilde{g}}, r_{\tilde{t}})$ are loop integrals. Each integral is

$$I_G(r_{\tilde{g}}, r_{\tilde{t}}) = \int_0^1 dx_1 \ldots dx_4 \delta(\Sigma_i x_i - 1) \times \frac{2x_1x_3x_4}{[r_{\tilde{g}}(x_1+x_2) + x_3 + r_{\tilde{t}}x_4]^4}, \tag{A3}$$

$$I_{S_1}(r_{\tilde{g}}, r_{\tilde{t}}) = \int_0^1 dx_1 \ldots dx_4 \delta(\Sigma_i x_i - 1) \times \frac{(2x_3 + 2x_4 - 1)x_3x_4}{[r_{\tilde{g}}x_1 + x_2 + x_3 + r_{\tilde{t}}x_4]^4}, \tag{A4}$$

$$I_{S_2}(r_{\tilde{g}}, r_{\tilde{t}}) = \int_0^1 dx_1 \ldots dx_5 \delta(\Sigma_i x_i - 1) \times \frac{(2x_3 + 2x_5 - 1)x_5}{[r_{\tilde{g}}x_1 + x_2 + x_3 + r_{\tilde{t}}(x_4 + x_5)]^4}, \tag{A5}$$

$$I_{S_3}(r_{\tilde{g}}, r_{\tilde{t}}) = \int_0^1 dx_1 \ldots dx_5 \delta(\Sigma_i x_i - 1) \times \frac{(2x_3 + 2x_5 - 1)x_4}{[r_{\tilde{g}}x_1 + x_2 + x_3 + r_{\tilde{t}}(x_4 + x_5)]^4}, \tag{A6}$$

$$I_{S_4}(r_{\tilde{g}}, r_{\tilde{t}}) = \int_0^1 dx_1 \ldots dx_4 \delta(\Sigma_i x_i - 1) \times \frac{(2x_3 - 1)x_2x_4}{[r_{\tilde{g}}x_1 + x_2 + x_3 + r_{\tilde{t}}x_4]^4}. \tag{A7}$$

We show the values of $F_{\rm MIA}(r_{\tilde{g}}, r_{\tilde{t}})$ with several values of mass ratio, $r_{\tilde{g}}$ and $r_{\tilde{t}}$ (see Table V).

[1] H. Georgi and S. L. Glashow, Phys. Rev. Lett. **32**, 438 (1974).

[2] F. Gabbiani, E. Gabrielli, A. Masiero, and L. Silvestrini, Nucl. Phys. **B477**, 321 (1996).

[3] G. Aad *et al.* (ATLAS Collaboration), Phys. Lett. B **716**, 1 (2012); S. Chatrchyan *et al.* (CMS Collaboration), Phys. Lett. B **716**, 30 (2012).

[4] N. Arkani-Hamed and S. Dimopoulos, J. High Energy Phys. 06 (2005) 073; G. F. Giudice and A. Romanino, Nucl. Phys. **B699**, 65 (2004); **B706**, 487 (2005); N. Arkani-Hamed, S. Dimopoulos, G. F. Giudice, and A. Romanino, Nucl. Phys. **B709**, 3 (2005); J. D. Wells, Phys. Rev. D **71**, 015013 (2005); G. F. Giudice and A. Strumia, Nucl. Phys. **B858**, 63 (2012); L. J. Hall and Y. Nomura, J. High Energy Phys. 01 (2012) 082; M. Ibe and T. T. Yanagida, Phys. Lett. B **709**, 374 (2012); M. Ibe, S. Matsumoto, and T. T. Yanagida, Phys. Rev. D **85**, 095011 (2012); N. Arkani-Hamed, A. Gupta, D. E. Kaplan, N. Weiner, and T. Zorawski, arXiv:1212.6971.

[5] S. Dimopoulos and G. Giudice, Phys. Lett. B **357**, 573 (1995); A. Pomarol and D. Tommasini, Nucl. Phys. **B466**, 3

(1996); A. Cohen, D. Kaplan, and A. Nelson, Phys. Lett. B **388**, 588 (1996); N. Arkani-Hamed and H. Murayama, Phys. Rev. D **56**, R6733 (1997); J. Hisano, K. Kurosawa, and Y. Nomura, Nucl. Phys. **B584**, 3 (2000).

[6] N. Maekawa, Phys. Lett. B **561**, 273 (2003); Prog. Theor. Phys. **112**, 639 (2004).

[7] K. Hamaguchi, M. Kakizaki, and M. Yamaguchi, Phys. Rev. D **68**, 056007 (2003).

[8] H. Fritzsch and P. Minkowski, Ann. Phys. (N.Y.) **93**, 193 (1975); F. Gursey, P. Ramond, and P. Sikivie, Phys. Lett. **60B**, 177 (1976); Y. Achiman and B. Stech, Phys. Lett. **77B**, 389 (1978); R. Barbieri and D. V. Nanopoulos, Phys. Lett. **91B**, 369 (1980).

[9] T. Kugo and J. Sato, Prog. Theor. Phys. **91**, 1217 (1994); N. Irges, S. Lavignac, and P. Ramond, Phys. Rev. D **58**, 035003 (1998); M. Bando and T. Kugo, Prog. Theor. Phys. **101**, 1313 (1999); M. Bando, T. Kugo, and K. Yoshioka, Prog. Theor. Phys. **104**, 211 (2000).

[10] M. Bando and N. Maekawa, Prog. Theor. Phys. **106**, 1255 (2001); N. Maekawa and T. Yamashita, Prog. Theor. Phys. **107**, 1201 (2002).

[11] N. Maekawa, Prog. Theor. Phys. **106**, 401 (2001); **107**, 597 (2002).

[12] S.-G. Kim, N. Maekawa, A. Matsuzaki, K. Sakurai, and T. Yoshikawa, Phys. Rev. D **75**, 115008 (2007); Prog. Theor. Phys. **121**, 49 (2009).

[13] J. M. Pendlebury *et al.*, Phys. Rev. D **92**, 092003 (2015); B. Graner, Y. Chen, E. G. Lindahl, and B. R. Heckel, Phys. Rev. Lett. **116**, 161601 (2016).

[14] S. Dimopoulos and L. J. Hall, Phys. Lett. B **344**, 185 (1995); J. Hisano and Y. Shimizu, Phys. Rev. D **70**, 093001 (2004).

[15] M. Ishiduki, S.-G. Kim, N. Maekawa, and K. Sakurai, Prog. Theor. Phys. **122**, 659 (2009); F. Sala, J. High Energy Phys. 03 (2014) 061.

[16] L. J. Hall, V. A. Kostelecky, and S. Raby, Nucl. Phys. **B267**, 415 (1986).

[17] K. Fuyuto, J. Hisano, and N. Nagata, Phys. Rev. D **87**, 054018 (2013).

[18] M. Jung and A. Pich, J. High Energy Phys. 04 (2014) 076.

[19] J. Engel, M. J. Ramsey-Musolf, and U. van Kolck, Prog. Part. Nucl. Phys. **71**, 21 (2013).

[20] M. Ishiduki, S.-G. Kim, N. Maekawa, and K. Sakurai, Phys. Rev. D **80**, 115011 (2009); **81**, 039901(E) (2010); H. Kawase and N. Maekawa, Prog. Theor. Phys. **123**, 941 (2010); N. Maekawa and K. Takayama, Phys. Rev. D **85**, 095015 (2012).

[21] Y. Nakai and M. Reece, arXiv:1612.08090.

[22] S. P. Martin and Michael T. Vaughn, Phys. Rev. D **50**, 2282 (1994).

[23] C. D. Froggatt and H. B. Nielsen, Nucl. Phys. **B147**, 277 (1979); L. E. Ibanez and G. G. Ross, Phys. Lett. B **332**, 100 (1994).

[24] K. Bodek *et al.*, arXiv:0806.4837; I. Altarev *et al.*, Nucl. Instrum. Methods Phys. Res., Sect. A **611**, 133 (2009); C. A. Baker *et al.*, J. Phys. Conf. Ser. **251**, 012055 (2010); D. H. Beck *et al.* (nEDM Collaboration), arXiv:1111.1273; I. Altarev *et al.*, Nuovo Cimento Soc. Ital. Fis., C **035N04**, 122 (2012).

[25] S. Heinemeyer, W. Hollik, and G. Weiglein, Eur. Phys. J. C **9**, 343 (1999); Comput. Phys. Commun. **124**, 76 (2000); G. Degrassi, S. Heinemeyer, W. Hollik, P. Slavich, and G. Weiglein, Eur. Phys. J. C **28**, 133 (2003); M. Frank, T. Hahn, S. Heinemeyer, W. Hollik, H. Rzehak, and G. Weiglein, J. High Energy Phys. 02 (2007) 047; T. Hahn, S. Heinemeyer, W. Hollik, H. Rzehak, and G. Weiglein, Comput. Phys. Commun. **180**, 1426 (2009). See http://www.feynhiggs.de.

[26] J. Baron *et al.* (ACME Collaboration), Science **343**, 269 (2014).

[27] J. Ellis, J. S. Lee, and A. Pilaftsis, J. High Energy Phys. 10 (2008) 049.

[28] T. Chupp and M. Ramsey-Musolf, Phys. Rev. C **91**, 035502 (2015); J. Doyle, http://online.kitp.ucsb.edu/online/nuclear_c16/doyle/.